Structure Sensitive Adsorption of DMSO on Au Surfaces

Norihito Ikemiya and Andrew A. Gewirth*

Department of Chemistry and Frederick Seitz Materials Research Laboratory, University of Illinois at Urbana-Champaign, Urbana, IL 61801

Received: December 3, 1999

Using a variable temperature STM, we have observed the adsorption of DMSO on Au(100) and Au(111) surfaces at temperatures below 215 K. For DMSO on Au(100), the molecules are trapped on the terraces at high points on the hex reconstruction giving rise to an ordered low coverage phase. Consistent with data from previous temperature programmed desorption (TPD) measurements, this phase coexists with a higher coverage "striped" phase formed when the DMSO molecules associate with each other. On Au(111), the DMSO molecules nucleate, order, and grow only from step edges; the steps are the only appropriately electropositive sites on this surface.

I. Introduction

There is considerable interest in the structure of solvents on surfaces for many reasons. Many electrochemical phenomena have their origin in the structure of the solid−liquid interface. Most importantly, there is a growing appreciation that solvent-ordering, both laterally and normal to the plane, plays an important role in informing properties of the electrochemical double layer. Indeed, Grahame invoked an "ice-like" layer in some of his discussion of the application of the Gouy−Chapman model to the Hg/solution interface.[1]

Before more general questions concerning the structure of the solvent−electrolyte complex can be addressed, it is important to understand the way in which simple solvents interact with metal surfaces on their own. There has been a long-standing interest in understanding the way in which water adsorbs on metals,[2−4] but relatively little effort has been expended for other solvents. The interaction of solvents with conductive, typically metallic, surfaces forms the basis for much of electrochemistry. This interaction, when combined with an appropriate electrolyte, leads to the formation of the electrochemical double layer. Adsorption of solvents onto electrode surfaces in electrolyte solutions has long been investigated to elucidate the nature of the solid−liquid interface.[5]

In this paper, we report the results of low-temperature ultrahigh vacuum (UHV) scanning tunneling microscopy (STM) measurements examining the adsorption of dimethylsulfoxide [$(CH_3)_2S{=}O$; DMSO] on the reconstructed Au(111) and Au-(100) single-crystal surfaces. Like water, DMSO is an important solvent in electrochemistry and its properties at electrode surfaces have long been studied.[6−9] DMSO has been the focus of intense study because of its self-associative properties in neat solution,[10−15] mixed with water,[16,17] and mixed with other solvents.[18,19] The DMSO molecule finds use as an anti-inflammatory agent, as a cryoprotectant, and as a free-radical scavenger in cancer treatments.[20] The structure of the water−DMSO interface has recently been probed because of the importance of the molecule in atmospheric chemistry.[16,21]

UHV-based techniques have examined the behavior of DMSO on Pt(111)[22−24] and Au(100).[25,26] On Pt(111), DMSO exhibits a (2 × 2) LEED pattern in the lowest coverage regime and the molecule is thought to associate with this surface primarily through the S atom. On Au(100) DMSO exhibits two correlated monolayer-related desorption peaks which suggests that it has two different low coverage phases on this surface. On the basis of analysis of X-ray photoelectron spectroscopic (XPS) data, DMSO is thought to associate with gold via interactions from the lone pairs on both the S and O moieties. However, there is no information about either the structure adopted by DMSO on any Au surface, or about the mode of growth of this molecule from vapor-phase adsorption.

II. Experimental Section

Variable temperature UHV-STM measurements were obtained by using an Omicron VTSTM as described in an earlier report.[4] The tunneling tips were commercial Pt−Ir tips (Digital Instruments, Santa Barbara, CA). The Au(100) face was obtained by using an electropolished single crystal obtained from Monocrystals Company and oriented to within less than 1 degree. The Au(111) surfaces were obtained as Au films deposited on borosilicate glass (Dirk Schröer, Inc., Berlin). Both surfaces were prepared using sputter−anneal cycles. STM images were recorded in constant current mode with tunneling conditions as indicated in the figure captions.

DMSO (Aldrich, >99.8% anhydride, water <0.005%) was transferred into a small glass bottle under an Ar environment to prevent contamination and attached to a leak valve of the gas inlet system to the UHV chamber. It was cleaned and degassed by repeated freeze−thaw cycles. DMSO adsorption was performed by filling the chamber with DMSO to a pressure of 5×10^{-9} mbar for 2−5 min while maintaining the sample between 120 and 215 K. This procedure typically leads to a thick coverage (ca. 5−10 ML) of DMSO on the surface as determined by calculation assuming a sticking coefficient of unity and by direct observation with the STM which reveals a featureless surface much different from the initial clean surface after this exposure. Following deposition, all DMSO films were annealed at 200−220 K which is below the monolayer desorption peaks,[25,26] but above the temperature at which multilayer desorption occurs. STM observations were then performed at various temperatures between 50 and 215 K.

* Author to whom correspondence should be addressed. Telephone: 217-333-8329. Fax: 217-333-2685. E-mail: agewirth@uiuc.edu.

10.1021/jp994251+ CCC: $19.00
Published on Web 01/14/2000

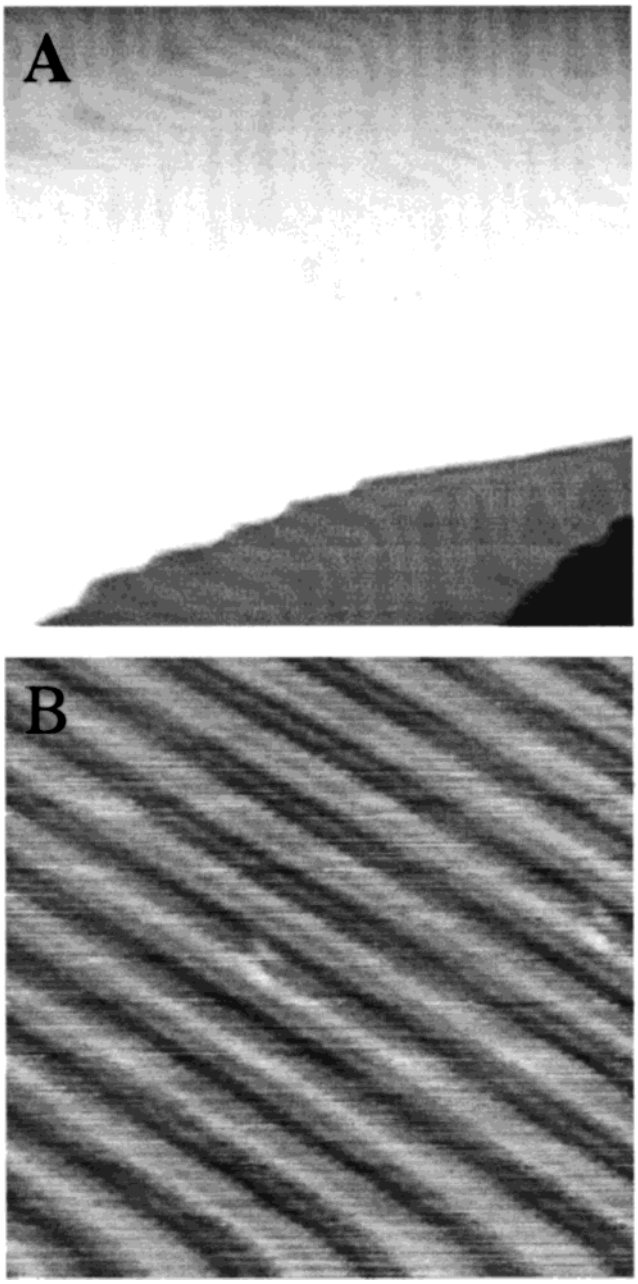

Figure 1. (A) 70 nm × 70 nm STM image of the Au(111) surface obtained at room temperature showing the ($\sqrt{3} \times 23$) reconstruction. $V_{tip} = -1.5$ V, $I_{tunnel} = 0.10$ nA; (B) 8 nm × 8 nm room temperature STM image of the reconstructed Au(100) surface showing the row structure characteristic of the (5 × 20) reconstruction. $V_{tip} = -1.39$ V, $I_{tunnel} = 0.83$ nA.

III. Results

Figure 1 shows STM images of the Au(111) (Figure 1A) and Au(100) (Figure 1B) surfaces showing the characteristic reconstructed structures[27−29] expected for the clean surfaces. A brief recapitulation of these surfaces follows. For Au(111), the ($\sqrt{3} \times 23$) reconstruction contains one extra atom per unit cell. This extra atom causes the surface to contract by 4% relative to the bulk in one of the three ⟨110⟩ directions, which causes every 23rd surface atom to be in registry with the underlying bulk atoms. The surface is described by areas of fcc and hcp registration with the underlying Au lattice. The dislocation faults between these two regions give rise to the characteristic "herringbone" pattern shown in Figure 1A. The Au(100) surface reconstructs into a cell of approximately (5 × 20), the driving force for which is to expose (111) facets which are at lower energy. The atomic density is approximately 20−25% higher in this top layer and along the ⟨110⟩ direction every fifth atomic row is bunched outward by approximately 0.1 nm. This gives rise to the characteristic row structures seen in Figure 1B.

A. Au(100). Initially, long-range images of the Au(100) surface obtained at low temperature revealed clean terraces interrupted by steps as shown in Figure 2A. Following exposure of Au(100) to DMSO and subsequent annealing of this surface to 220 K, two different structures were observed on the surface. The first of these, a low coverage structure, is shown in Figure 2B which was obtained at 165 K. The image shows many small islands which are dispersed on terraces as well as at step edges. Because these islands are not present in images obtained prior to DMSO exposure which show only terrace features on the length scale shown here, we associate these islands with DMSO adsorbed onto the Au(100) surface. These islands are planar and have an apparent height of 0.2 nm above the Au(100) surface, the structure of which is evident in smaller scale images between the islands. The height of this film above the surface was approximately 0.2 nm, which is smaller than the size expected from the molecular structure alone (about 0.3 nm).[30] However, it is well-understood that the apparent height of adsorbates and other features in STM images is strongly affected by the particular choice of imaging parameters and their interaction with electronic states in the adsorbate and the surface.[31,32] This image suggests that DMSO preferentially nucleates at sites on the Au(100) terrace and that molecularly high islands grow from these initial sites. That islands exist on the surface attests to what must be a strong self-associative preference for the DMSO molecule. This kind of phase behavior has been observed in a number of other molecular species as overlayer growth is followed, most notably the thiols on Au(111)[33] and has recently been the subject of a detailed scaling analysis[34,35] for films assembled onto mica.

We also observed a higher coverage phase for DMSO adsorbed onto Au(100) as shown in the STM image taken at 165 K given in Figure 2C. The figure shows a striped pattern formed by the adsorbed molecules. The width of the stripes varies from 2 to 10 nm, and the image shows that the length of the stripes is also quite variable. However, the spacing between the stripes (the dark lines) was much more consistent and equal to 1.4 ± 0.6 nm. This stripped pattern was found on terraces almost completely covered by DMSO. Higher resolution images showing molecular resolution were not obtained from this film for temperatures between 50 and 215 K. In some experiments, these structures were observed to coalesce into full monolayers of DMSO.

Molecular resolution from films of the type seen in Figure 2B was not obtained at 165 K. However, cooling the sample down to 65 K gave rise to images, an example of which is shown in Figure 3A, presumably by suppressing thermal motion of DMSO within the overlayer. The spacing between the rows of the features is 1.5 ± 0.1 nm which is the same as that between ridges of the reconstructed Au(100) surface which are in addition observed to be colinear with the rows. Along the rows, the spacing is 1.2 ± 0.1 nm and the primitive unit cell is oblique with an angle of 11 ± 4°. These spacings are consistent with a ($4 \times \sqrt{126}$)R11.3° unit cell. We note that the 1.5 nm spacing between the rows is the same as that formed by the reconstructed Au(100) surface itself. Outside these island structures the bare reconstructed Au(100) surface is imaged. This suggests that the ($4 \times \sqrt{126}$)R11.3° cell seen is not an artifact formed by a "Behm amplifier" or other anomaly. That this structure is seen

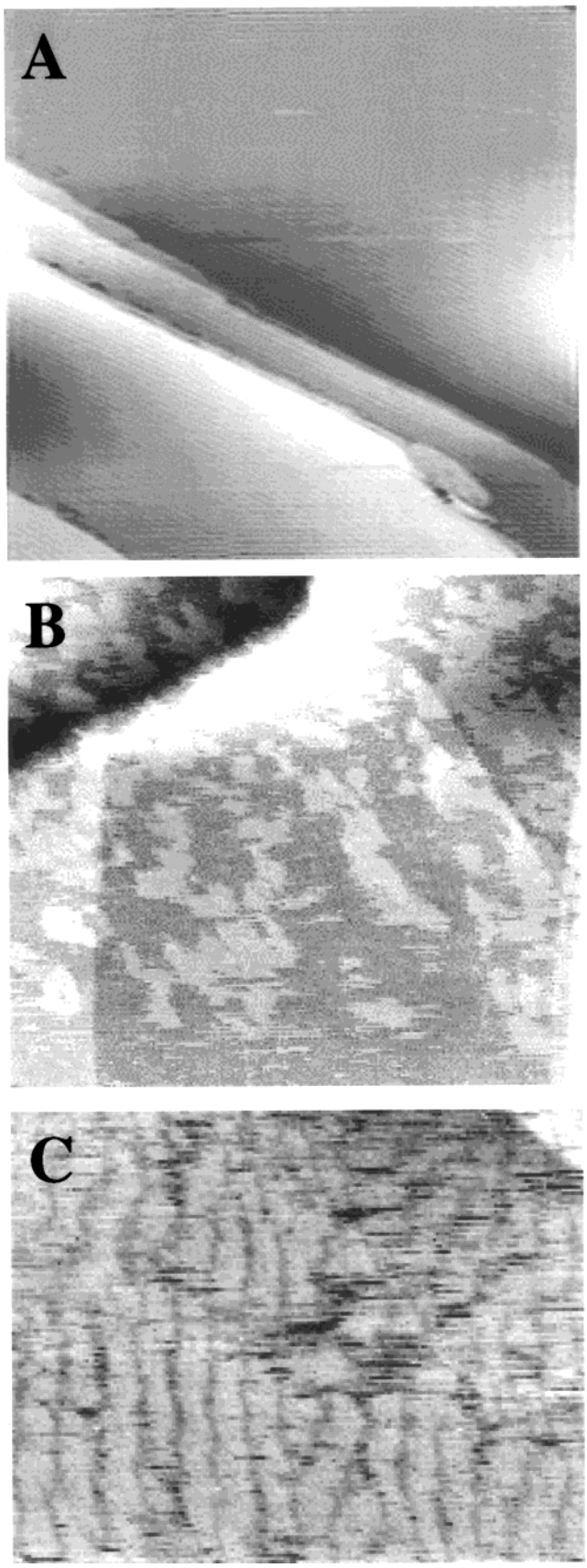

Figure 2. (A) 100 nm × 100 nm STM image of a bare Au(100) surface obtained at 190 K. The reconstruction rows are just visible on the terraces. (B) 147 nm × 132 nm STM image of low coverages of DMSO on Au(100) taken at 165 K. $V_{tip} = -1.5$ V, $I_{tunnel} = 0.1$ nA. (C) 114 nm × 90 nm STM image of the striped pattern of DMSO on Au(100) taken at 165 K. $V_{tip} = -1.5$ V, $I_{tunnel} = 0.06$ nA.

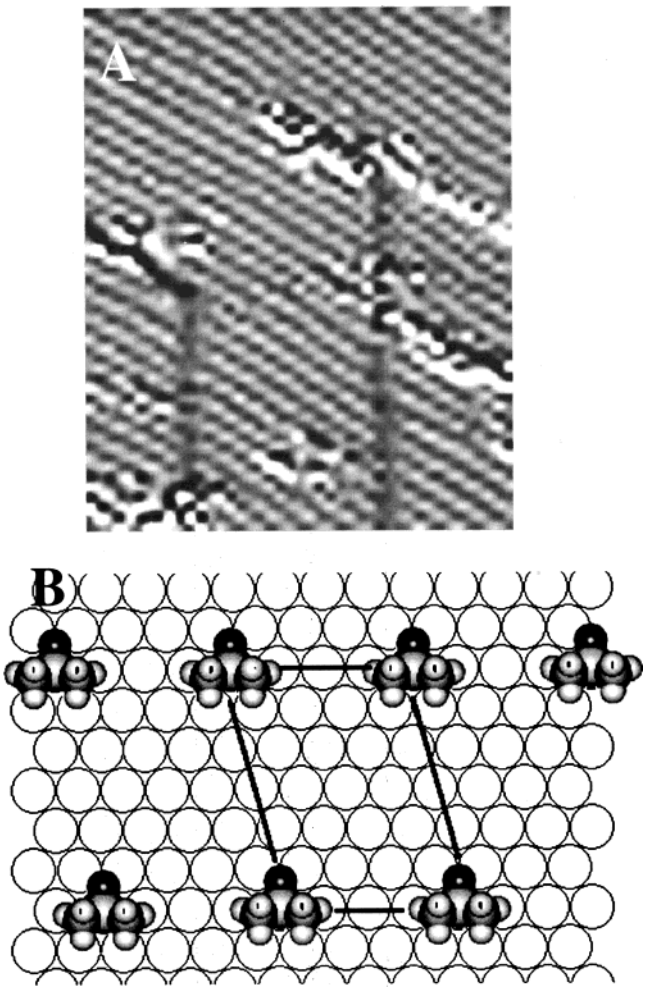

Figure 3. (A) 39 nm × 30 nm STM image of DMSO on Au(100) at 65 K. $V_{tip} = -1.5$V, $I_{tunnel} = 0.1$ nA. The image has been differentiated to more clearly show the molecular corrugation. (B) Model of the (4 × $\sqrt{26}$)R11.3° DMSO unit cell.

in small isolated islands suggest that it is the initial structure formed by DMSO as it impinges and diffuses before being trapped on the Au(100) surface.

Although the registry of DMSO is not determined in this study, a tentative structural model of the overlayer shown in Figure 3A is shown in Figure 3B. In this model, we assume an (S,O)-bidenate adsorption geometry of DMSO, which has been proposed from X-ray photoelectron spectroscopy (XPS) studies.[25,26] From the STM image, one adsorbed DMSO molecule occupies an area of about 1.7 nm^2, which is much less dense than the approximately 0.2 nm^2 evaluated from the projection of planes in the bulk crystal.[10] In the case of DMSO on Pt(111),[22−24] a much denser (2 × 2) DMSO structure (0.25 coverage) was found even at the initial stage of adsorption. This may arise as a consequence of what must be the considerably stronger affinity of DMSO for Pt relative to Au; the monolayer TPD peak occurs at 385 K on Pt and at 240 K on Au(100).

B. Au(111). On the (111) face of Au a completely different morphology of DMSO develops. Figure 4A shows a STM image of DMSO on Au(111) at 120 K. Clearly evident is the preferential decoration of both the upper side and lower side of step edges with DMSO molecules. At lower coverages than those shown here, we observe that DMSO exclusively decorates the upper side of the step edges and forms one-dimensional chain structures. The image shows that the DMSO layers start to grow from the step edges and merge in the centers of the

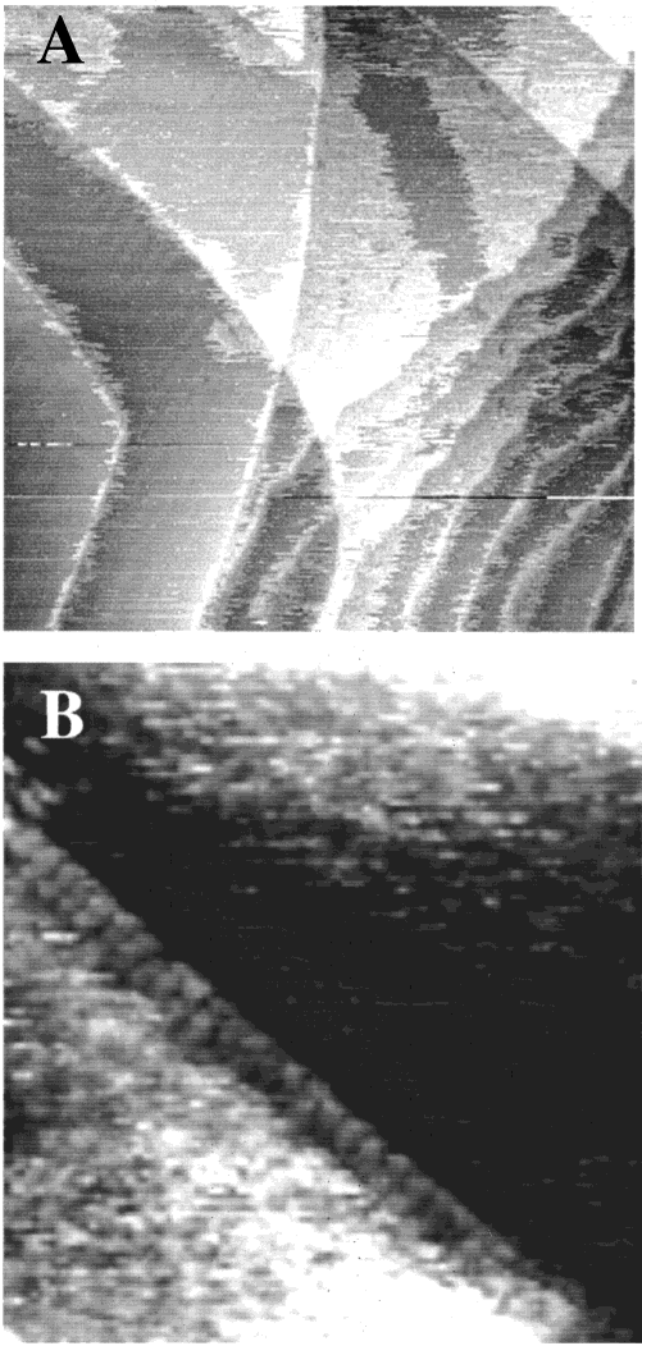

Figure 4. (A) 148 nm × 148 nm STM image of DMSO on Au(111) at 120 K. $V_{tip} = -2.1$V, $I_{tunnel} = 0.1$ nA. (B) 55 nm × 59 nm STM image of DMSO on Au(111) at 55 K. $V_{tip} = 2.0$ V, $I_{tunnel} = 0.1$ nA.

terraces. Moreover, we have never seen DMSO islands nucleated directly on terraces in contrast to what occurs on the more highly corrugated Au(100) surface. The reconstructed Au(111) surface is still apparent in these images, suggesting that on this face as well the reconstruction is not lifted by the DMSO adsorbate.

No long-range ordered structures were observed on terraces even at 55 K. However, we did observe a regularly arranged pattern at step edges as shown in Figure 4B. The image in Figure 4B shows a linear array of an ordered structure decorating the top of one of the step edges of the Au(111) surface. The spacing between the oblong features is approximately 2 nm. There were no suggestions of molecular order below the step edge or at any remove from the step. In particular, we did not see any evidence for the consequences of Friedel oscillations that have been described for benzene on Cu(111).[36] This may be a consequence of the high density of DMSO already on the terraces in the images we were able to obtain.

IV. Discussion

The images shown above provide insight into the way in which DMSO interacts with Au surfaces.

First, we observe two different submonolayer coverage phases for DMSO on the reconstructed Au(100) surface. These two phases were observed to coexist with each other and the more dense phase was observed to coalesce into what appeared to be a full monolayer of DMSO. The existence of two types of DMSO morphologies observed here corroborate recent temperature-programmed desorption (TPD) data[25,26] which showed that DMSO desorbs from two distinct yet correlated states at 240 and 275 K. Since both the high and low coverage phases are present at the same time on the surface in our measurements, we suggest that these correlate with the β_1 and β_2 TPD phases seen by Solomun and coworkers.

While the less dense layer of DMSO is observed to relate to specific sites of the Au(100) reconstruction, the more densely packed striped phase has no such easy relationship with the surface. The highly variable width of the overlayer stripes suggests that they form as a consequence of a two-dimensional condensation process wherein attractive interactions between DMSO molecules come in to play. DMSO is known to self-associate in bulk solution[12] and a number of different oligimeric motifs have been reported. A combination of these motifs may be responsible for the aggregation seen here.

By the same token, the space between the stripes is formed as a consequence of some sort of repulsion between the layers. What could be the origin of this repulsion? Because the lamella don't appear to follow any crystallographic feature of the underlying surface, and because it is known that the Au(100) reconstruction is not removed by DMSO adsorption, the substrate is likely not the source of this repulsion. We thus look to the DMSO itself. In bulk solution, DMSO is thought to form a series of chains with the molecular dipoles of neighboring molecules lying roughly antiparallel to each other,[12] although the extent of association between molecules has been questioned.[15] A defect of about three molecules in width would account for the spacing seen in this study which might result from a phase mismatch between lamella. We have seen such defects at high resolution in STM images obtained in ambient conditions from bulk DMSO solutions on Au surfaces.[37] More detailed measurements must be performed to confirm this speculation.

Another striking result from our STM investigation is the observation of different modes of growth for DMSO on different Au faces. This must relate to different initial nucleation sites between the two faces of Au. The mode of adsorption of DMSO we observe on Au(111) is consistent with that observed for other molecules such as benzene on Cu(111)[36,38] and C_{60} on both Au(111)[39−42] and Cu(111).[43] The trapping of DMSO molecules at step edges arises from the enhanced adsorption probability at step edges of Au(111).[44] The origin of this enhanced trapping probability is likely electronic in origin, as the upper step edge is preferentially decorated. Moreover, the observation of order on the upper step edge suggests that the site is able to pin the DMSO molecule in a preferential orientation. This is not true at the lower step edge.

On Au(100), the molecules show affinity for the terraces and form an ordered molecular array which follows the texture of the reconstruction lines on this surface. Strong interaction between C_{60} and the Au(100) hex reconstruction has also been

observed,[45] and between C_{60} and the correspondingly reconstructed Au(110) surface.[46] DMSO associates with Au via a weak charge transfer from lone pairs on the S and O bond to the Au surface. This charge transfer will undoubtedly be enhanced at electropositive sites on the surface. The nearly 0.1 nm-high Au surface atoms at the reconstruction kink sites on the Au(100) surface will be more electropositive than their neighbors which are not elevated above the plane. Likewise, the upper step edge on the Au(111) surface provides an electropositive site for adsorption.

These considerations suggest that control of the initial sites of adsorption of DMSO on Au surfaces is afforded by the electronic structure of the Au surface. The different degree of charge localized to different sites on the surface affects the initial stages of growth of the molecular film. We are in the process of exploring consequences of the different mode of association on the properties of the DMSO liquid−solid interface.

Acknowledgment. The assistance of Vania Petrova and the staff of the Center for the Microanalysis of Materials is gratefully acknowledged. This work was funded by Department of Energy Grant DE-FG02-91ER45349 through the Materials Research Laboratory at the University of Illinois. STM images were obtained in the Center for the Microanalysis of Materials at the University of Illinois, which is supported by Department of Energy Grant DE-FG02- 91ER45349.

References and Notes

(1) Bard, A. J.; Faulkner, L. R. *Electrochemical Methods*; John Wiley and Sons, Inc.: New York, 1980.
(2) Thiel, P. A.; Madey, T. E. *Surf. Sci. Rep.* **1987**, *7*, 21.
(3) Morgenstern, M.; Michely, T.; Comsa, G. *Phys. Rev. Lett.* **1996**, *77*, 703−706.
(4) Ikemiya, N.; Gewirth, A. A. *J. Am. Chem. Soc.* **1997**, *119*, 9919−9920.
(5) Lipkowski, J.; Ross, P. N. *Adsorption of Molecules at Metal Electrodes*; VCH Publishers: New York, 1992.
(6) Motheo, A. J.; Gonzalez, E. R. *Electrochim. Acta* **1996**, *41*, 2631−2638.
(7) Jarzabek, G.; Borkowska, Z. *J. Electroanal. Chem.* **1987**, *226*, 295−303.
(8) Jarzabek, G.; Borkowska, Z. *J. Electroanal. Chem.* **1988**, *248*, 399−410.
(9) Borkowska, Z.; Hamelin, A. *J. Electroanal. Chem.* **1988**, *241*, 373−377.
(10) Viswamitra, M. A.; Kannan, K. K. *Nature* **1966**, *209*, 1016.
(11) Bertagnolli, H.; Schultz, E.; Chieux, P. *Ber. Bunsen-Ges. Phys. Chem.* **1989**, *93*, 88−95.
(12) Itoh, S.; Ohtaki, H. *Z. Naturforsch.* **1987**, *A42*, 858.
(13) Berresheim, H.; Huey, J. W.; Thorn, R. P.; Eisele, F. L.; Tanner, D. J.; Jefferson, A. *J. Geophys. Res.* **1998**, *103*, 1629−1637.
(14) Forel, M.-T.; Tranquille, M. *Spectrochim. Acta* **1970**, *26A*, 1023−1034.
(15) Luzar, A.; Soper, A. K.; Chandler, D. *J. Chem. Phys.* **1993**, *99*, 6836−6847.
(16) Karpovich, D. S.; Ray, D. *J. Phys. Chem. B* **1998**, *102*, 649−652.
(17) Vaisman, I. I.; Berkowitz, M. L. *J. Am. Chem. Soc.* **1992**, *114*, 7889−7896.
(18) Kinart, C. M.; Kinart, W. J. *Phys. Chem. Liq.* **1995**, *29*, 1−7.
(19) Fawcett, W. R.; Kloss, A. A. *J. Chem. Soc. Faraday Trans.* **1996**, *92*, 3333.
(20) Jacob, S. W.; Rosenbaum, E. E.; Wood, D. C. *Dimethyl Sulfoxide*; Marcel Dekker, Inc.: New York, 1971; Vol. 1.
(21) Allen, H. C.; Gragson, D. E.; Richmond, G. L. *J Phys. Chem. B* **1999**, *103*, 660−666.
(22) Garwood, G. A.; Hubbard, A. T. *Surf. Sci.* **1982**, *118*, 223.
(23) Sexton, B. A.; Avery, N. R.; Turney, T. W. *Surf. Sci.* **1983**, *124*, 162.
(24) Katekaru, J. K.; Garwood, J. G. A.; Hershberger, J. F.; Hubbard, A. T. *Surf. Sci.* **1982**, *121*, 396.
(25) Schroter, C.; Roelfs, B.; Solomun, T. *Surf. Sci.* **1997**, *380*, L441.
(26) Roelfs, B.; Schroter, C.; Solomun, T. *Ber. Bunsen-Ges. Phys. Chem.* **1997**, *101*, 1105−1112.
(27) Woll, C.; Chiang, S.; Wilson, R. J.; Lippel, P. H. *Phys. Rev. B* **1989**, *39*, 7988.
(28) Barth, J. V.; Brune, H.; Ertl, H.; Behm, R. J. *Phys. Rev. B* **1990**, *42*, 9307.
(29) Barth, J. V.; Schuster, R.; Behm, R. J.; Ertl, G. *Surf. Sci.* **1994**, *302*, 158−170.
(30) Thomas, R.; Shoemaker, C. B.; Eriks, K. *Acta Cryst.* **1996**, *21*, 12.
(31) Morgenstern, M.; Muller, J.; Michely, T.; Comsa, G. *Z. Phys. Chem.* **1997**, *198*, 43−72.
(32) Sautet, P. *Chem. Rev.* **1997**, *97*, 1097−1116.
(33) Poirier, G. E.; Pylant, E. D. *Science* **1996**, *272*, 1145.
(34) Doudevski, I.; Hayes, W. A.; Schwartz, D. K. *Phys. Rev. Lett.* **1998**, *81*, 4927−4930.
(35) Doudevski, I.; Schwartz, D. K. *Phys. Rev. B* **1999**, *60*, 14−17.
(36) Stranick, S. J.; Kamna, M. M.; Weiss, P. S. *Surf. Sci.* **1995**, *338*, 41−59.
(37) Si, S. K.; Gewirth, A. A. *Manuscript in preparation.*
(38) Stranick, S. J.; Kamna, M. M.; Weiss, P. S. *Science* **1994**, *266*, 99−102.
(39) Altman, E. I.; Colton, R. J. *Phys. Rev. B* **1993**, *48*, 18244.
(40) Altman, E. I.; Colton, R. J. *Surf. Sci.* **1993**, *295*, 13.
(41) Altman, E. I.; Colton, R. J. *Surf. Sci.* **1992**, *279*, 49.
(42) Fujita, D.; Yakabe, T.; Nejoh, H.; Sato, T.; Iwatsuki, M. *Surf. Sci.* **1996**, *366*, 93.
(43) Hashizume, T.; Sakurai, T. *J. Vac. Sci. Technol. B* **1994**, *12*, 1992.
(44) Hasegawa, Y.; Avouris, P. *Phys. Rev. Lett.* **1993**, *71*, 1071.
(45) Kuk, Y.; Kim, D. K.; Suh, Y. D.; Park, K. H.; Noh, H. P.; Oh, S. J.; Kim, S. K. *Phys. Rev. Lett.* **1993**, *70*, 1948.
(46) Modesti, S.; Gimzewski, J. K.; Schlittler, R. R. *Sulf. Sci.* **1995**, *333*, 1129−1135.